Key Points:

- North Atlantic cold-water corals trace well-ventilated thermocline waters near major oceanic fronts since the Last Glacial Maximum
- Across the South Atlantic into the Southern Ocean, aged waters with large variability and connectivity are evident during the last glacial
- The modern state of radiocarbon ventilation of the thermocline Atlantic is initiated during the Younger Dryas cold reversal

Correspondence to:

E. Beisel,
ebeisel@iup.uni-heidelberg.de

Climate Induced Thermocline Aging and Ventilation in the Eastern Atlantic Over the Last 32,000 Years

Elvira Beisel[1], Norbert Frank[1], Laura F. Robinson[2], Marleen Lausecker[1,3], Ronny Friedrich[4], Steffen Therre[1], Andrea Schröder-Ritzrau[1], and Martin Butzin[5]

[1]Institute of Environmental Physics, Heidelberg University, Heidelberg, Germany, [2]School of Earth Sciences, University of Bristol, Bristol, UK, [3]Alfred Wegener Institute, Helmholtz Centre for Polar and Marine Research, Bremerhaven, Germany, [4]Curt-Engelhorn-Center Archaeometry Mannheim, Mannheim, Germany, [5]MARUM-Center for Marine Environmental Sciences, University of Bremen, Bremen, Germany

Abstract The radiocarbon analysis of uranium-thorium-dated cold-water corals (CWCs) provides an excellent opportunity for qualitative reconstruction of past ocean circulation and water mass aging. While mid-depth water mass aging has been studied in the Atlantic Ocean, the evolution of the thermocline is still largely unknown. Here we present a combined ^{14}C and ^{230}Th/U age record obtained from thermocline dwelling CWCs at various sites in the eastern Atlantic Ocean, with intermittently centennial resolution over the last 32 ka. Shallow dwelling CWCs off Angola, located in the South Atlantic, infer a link between the mid-depth equatorial Atlantic and Southern Ocean. They confirm a ^{14}C drawdown during the Last Glacial Maximum (LGM) and advocate for a consistent Southern Hemisphere radiocarbon aging of upper thermocline waters, as well as strong depth gradients and high variability. Direct comparison with ^{14}C simulations carried out with an Ocean General Circulation Model yield good agreement for Angola. In contrast, the North Atlantic thermocline shows well-ventilated water with strong variations near the position of today's Azores Front (AF), neither of which are captured by the model. During the Bølling-Allerød, we confirm the important role of the AF in separating North and South Atlantic thermocline waters and provide further evidence of a 500 year long deep convection interruption within the Younger Dryas (YD). We conclude that the North and South Atlantic thermocline waters were separately acting carbon reservoirs during the LGM and subsequent deglaciation until the modern circulation was established during the YD.

1. Introduction

The Atlantic overturning circulation plays a crucial role in the transfer and storage of carbon across latitudes and thus determines the ventilation state. The term "ventilation" refers to "the collective effect of the physical and chemical processes that convey atmospheric properties into the ocean interior" (definition after Skinner and Bard (2022)). During the climate transition from the Last Glacial Maximum (LGM) to its modern strong circulation state, the overturning depth and its volume flux likely increased when compared to the glacial, probably shoaled circulation (e.g., Adkins, 2013; Bradtmiller et al., 2014). In addition, some studies suggest mainly two circulation cells, with presumably low mixing in between (Adkins, 2013; Lund et al., 2011). The Atlantic is a vital carbon reservoir, in which small changes in ocean-atmosphere exchange and wind forcing impact the atmospheric partial pressure of CO_2 (pCO$_2$, Barnola et al., 1987; Petit et al., 1999; Sigman & Boyle, 2000). The thermocline responds to atmospheric forcing via wind driven eddy flow and provides a way to store water properties such as dissolved carbon over decades to centuries (Lozier, 1997). Consequently, the Atlantic thermocline is a fast-acting part of the global marine carbon reservoir, barely studied for its ventilation history. A detailed reconstruction of ^{14}C ventilation ages is essential to fully reconstruct the spatiotemporal variability of Atlantic interior ventilation. Cold-water corals (CWCs) provide the means to establish high-resolution and high-precision records of the thermocline ventilation of the past. Their aragonite skeleton traps trace elements of surrounding water as they grow, allowing ^{230}Th/U dating (Smith et al., 1997) for absolute age determination. This provides absolute time scales allowing to resolve past seawater dissolved inorganic carbon ^{14}C levels through combined ^{230}Th/U and ^{14}C dating (Adkins et al., 1998; Frank et al., 2004; Mangini et al., 1998). The resulting age difference between the ocean and the contemporaneous atmosphere, that is, the Benthic-Atmosphere (B_{atm}) ages (Skinner & Bard, 2022), are valuable indicators of the Atlantic interior water mass advection pathways, and thus provide the key to reconstruct the prevailing circulation.
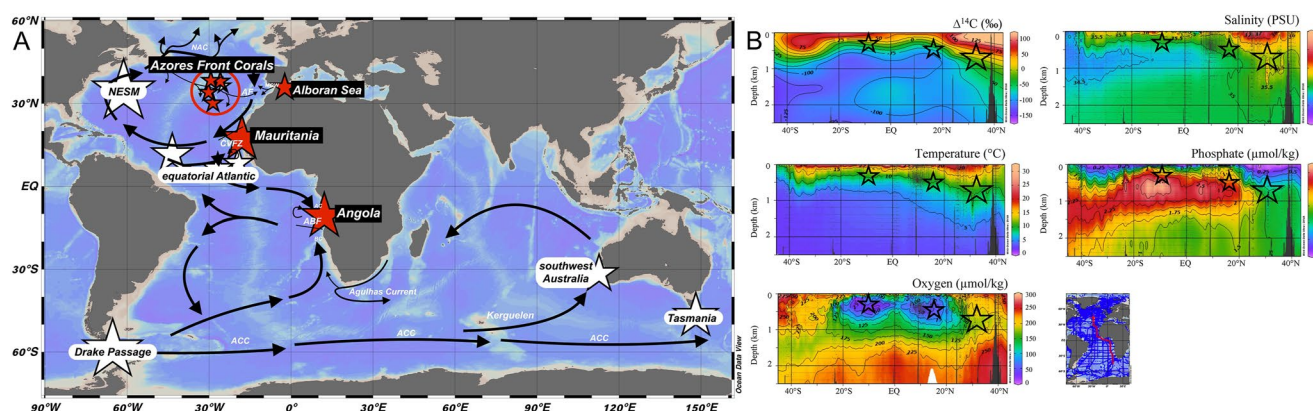
Figure 1. (a) Map of investigated sites, including major surface currents and fronts, as well as locations of previously published radiocarbon results using cold-water corals (CWC). Four new datasets are presented here (red stars): Alboran Sea (∼330 m), Azores Front Corals (AFC; Azores and Great Meteor Seamount region; 560–970 m), Mauritania (492–580 m) and Angola (259–457 m). Alboran Sea CWCs reveal the influence of Mediterranean Outflow Water in the Atlantic, where it nowadays influences AFC near the present-day AF. The CWCs off Mauritania are located near the Cap Verde Frontal Zone, while those off Angola are situated near the Angola-Benguela-Front. The Benguela Current carries water from the Antarctic Circumpolar Current and Agulhas Current, while the Angola Current flows southward. Our observations are compared to previously published CWC results (white stars) from the New England Seamount (Adkins et al., 1998; Eltgroth et al., 2006; Hines et al., 2019; Robinson et al., 2005; Thiagarajan et al., 2014), equatorial Atlantic (Chen et al., 2015, 2020), Drake Passage (Burke & Robinson, 2012; Chen et al., 2015; Li et al., 2020), southwest Australia (Trotter et al., 2022) and Tasmania (Hines et al., 2015). (b) Hydrography around sample locations. Black stars mark sampled areas. Figure created using Ocean Data View (Schlitzer, 2023).

While several studies suggest two distinct meridional overturning circulation cells in the Atlantic during the LGM (Adkins, 2013; Lund et al., 2011), the growing number of radiocarbon studies provides constrains on the ventilation state and thus vertical extension of these cells. First evidence of past mid-depth circulation changes and water mass aging in the Atlantic Ocean were collected using intermediate to deep dwelling CWCs and foraminifera (e.g., Chen et al., 2015; Eltgroth et al., 2006; Frank et al., 2004; Freeman et al., 2016; Keigwin & Schlegel, 2002; Mangini et al., 2010; Robinson et al., 2005; Schröder-Ritzrau et al., 2003; Skinner et al., 2014, 2021). Numerous radiocarbon records across the deep and South Atlantic showed significant aging, with a highest reservoir age increase in the mid-depth ocean of up to ∼2,500 years (Rafter et al., 2022; Skinner & Bard, 2022). Two different reasons, or a combination of both, may account for the interior water mass aging: (a) a reduced interior circulation, hence longer turn-over times for water, or (b) a reduction in air-sea gas exchange in deep-water formation regions at high-latitudes (Schmittner, 2003; Skinner & Bard, 2022). Both processes are well attested, with the global sea ice cover expanding during the last glacial (WAIS, 2015) and periods of reduced Atlantic Meridional Overturning Circulation (AMOC), as attested in numerous studies (Böhm et al., 2015). Furthermore, a variety of studies suggests a shallow, well-ventilated water mass with fast overturning in the North Atlantic during the LGM (e.g., Böhm et al., 2015; Chen et al., 2015; Cléroux et al., 2011; Freeman et al., 2016; Lippold et al., 2012; Skinner et al., 2017; Slowey & Curry, 1992). However, previous radiocarbon reconstructions above 1,000 m depth in the North Atlantic are derived mostly from foraminifera and show large scatter, ranging from very well-ventilated waters to strongly depleted waters with B_{atm} ages of up to 2,000 years (compilation by Skinner and Bard (2022)). As stated by Skinner and Bard (2022), one outstanding challenge for the interpretation of radiocarbon as ventilation age tracer is to narrow down the observed scatter in marine radiocarbon reservoir age estimates.

[230]Th/U dated CWCs overcome some of the impediments associated with the use of foraminifera (Skinner & Bard, 2022), and provide ventilation ages with higher precision regarding the absolute age determination and reservoir age uncertainty. Here, we study this part of the Atlantic thermocline ocean using framework forming CWCs to retrieve the evolution of the east Atlantic north-south ventilation difference since the last glacial. In addition, we test the regional consistency of available ventilation age observations from deep dwelling corals, which permit to infer a strong Southern Hemisphere connectivity of aged water masses and its upper age limit relevant for calibration purposes. We present four new $\Delta^{14}C$ datasets obtained on a total of 122 CWCs, which dwelled between 259 and 970 m depth at hydrographically important locations in the central and east Atlantic Ocean (Azores Front Corals (AFC), Mauritania, and Angola) as well as in the Alboran Sea (Figure 1). We compare our observations to ^{14}C simulation results and find good agreement for most of the Atlantic, whereas differences between model results and observations appear most significant for the North Atlantic north of the Azores Front (AF) and Mauritania during the last glacial.

2. Materials and Methods

2.1. Sites and Hydrography

Corals from 33 individual sites representing four distinct regions were selected for this study: (a) Alboran Sea, at the entrance/exit of the Mediterranean Sea, (b) Azores and Great Meteor Seamount, summarized under the term "AFC" and positioned near todays meandering AF, (c) offshore Mauritania in the subtropical North Atlantic, and (d) offshore Angola in the subtropical South Atlantic (Figure 1). Corals were recovered using a variety of equipment, including remotely operated vehicles, gravity corers and grab samplers. Predominantly framework forming species such as *Desmophyllum pertusum* (formerly known as *Lophelia pertusa*) and *Madrepora oculata* were selected, with a few solitary species such as *Desmophyllum dianthus*. Corals were well preserved, with occasional minor traces of bioerosion and coating, that were removed through mechanical cleaning. The selected sites reflect a slightly uneven depth distribution with a median depth of 600 ± 250 m. Alboran Sea, Mauretania, and Angola represent depth intervals of 300–500 m, whereas the various sites near the Azores and Great Meteor Seamount reflect deeper habitats at 600–970 m. However, the sites are strongly connected via the thermocline water circulation (see below).

To determine the radiocarbon contribution of Mediterranean Outflow Water (MOW), we included corals from the Alboran Sea (35°N, 2°W). The Alboran Sea is directly connected to the North Atlantic Ocean via the inflow of Atlantic surface water due to the west-east sea surface height gradient from excess evaporation. Deep convection in the Mediterranean balances the flow with an outflow of warm and salty MOW into the North Atlantic. Given the short overturning time, these waters are today well-ventilated compared to the surrounding Atlantic waters. At 330 m depth within the Alboran Sea, $\Delta^{14}C$ reaches values of $+50‰$ today, which reflects the rapid overturning and thus bomb radiocarbon propagation from the Atlantic surface to the MOW. The selected corals were recovered at a depth of $\sim 330 \pm 6$ m from coral bearing gravity cores taken on the top of the Brittlestar coral mounds (Fentimen et al., 2020; Hebbeln et al., 2015; Krengel, 2020; Van Rooij et al., 2013), nowadays under persisted influence of MOW.

Further corals were selected from the Azores and Great Meteor Seamount region (29°N–38°N, 25°W–29°W, Figure 1a). They were recovered near the present-day AF by using a remotely operated vehicle (SQUID-MARUM) and a grab sampler. In this region, CWCs reflect singular occurrences instead of coral mounds (Frank et al., 2018). Today, the corals sites are mainly under the influence of Eastern North Atlantic water with a residual component of MOW (Frank et al., 2018; Palma et al., 2012). They are situated in a highly dynamic Atlantic frontal zone at the interface between subpolar and subtropical Atlantic waters, characterized by a strong latitudinal gradient of water mass properties. From south to north the nutrient concentration at upper thermocline depths decreases across the front by a factor of three, while oxygen increases by a factor of three (Figure 1b). Temperature and salinity increase with depth within the frontal zone due to Ekman pumping and heat and salt contributions from MOW, while north of the AF salinity and temperature decrease again. The downward flux of heat and carbon within the frontal zone is well attested through the penetration depth of bomb radiocarbon, which reaches $\Delta^{14}C$ values of $0‰$ in 800 m depth compared to $-50‰$ in pre-bomb times (Figure 1b). Here, we summarized the corals from this dynamic region under the term "AFC."

Our third site is situated off Mauritania (17°N–18°N, 16°W) (Westphal et al., 2014; Wienberg et al., 2018). The corals have been taken from five coral bearing gravity cores taken in one of the largest CWC provinces, known as the great wall of Mauritania (Wienberg et al., 2018). They periodically occur near the Cap Verde Frontal Zone (CVFZ), a region influenced by South Atlantic Central Water (SACW) with low oxygen concentrations and temperatures of 10–12°C (GLODAPv2.2022, Lauvset et al., 2021; Figure 1b). Therefore, the regions off Mauritania are nowadays predominantly characterized by a pronounced oxygen minimum zone, due to the sluggish recirculation and significant organic matter remineralization. The observed modern $\Delta^{14}C$ shows identical patterns to the ones off Angola, that is, slow downward penetration of bomb radiocarbon (Figure 1b).

Lastly, corals were studied from offshore Angola (9°S, 12°E), a major coral mound province (Hebbeln et al., 2017). CWCs were collected from three coral bearing sediment cores from two mounds, complemented by several coral fragments collected using a grab sampler and box corer. The sites are currently influenced by the southward flow of equatorial thermocline water through the Angola Current, and slow northeastward recirculation of subsurface waters from the Benguela Current. The pathways of advection strongly depend on the intensity of the Agulhas leakage at the southern tip of Africa (Veitch et al., 2010). The northward propagating SACW, and

possibly Antarctic Intermediate Water (AAIW), are injected into the thermocline underneath the Angola Dome upwelling system (Figure 1a). Water masses at the coral sites are today characterized by low oxygen contents of 25–50 μmol kg^{-1} and temperatures of 8–10°C, as well as high phosphate concentrations of >2.25 μmol kg^{-1} (GLODAPv2.2022, Lauvset et al., 2021; Figure 1b). According to Δ^{14}C observations collected as additional information by GLODAPv2.2022, Δ^{14}C ranges from −75‰ to +25‰ between 600 and 250 m depth, indicating an increase of Δ^{14}C of +100‰ in the upper most thermocline since the late 60s, while lower thermocline waters remain without influence of bomb-radiocarbon.

2.2. Uranium Series Dating and Selection Criteria

Solely well preserved CWC samples were selected based on precisely measured ^{230}Th/U, with ages of up to 32 ka. First, coral samples were thoroughly mechanically cleaned using a Dremel tool. U and Th were extracted according to the manual method of Wefing et al. (2017). The high precision isotopic measurements were performed on a multi-collector inductively coupled plasma mass spectrometer (MC-ICP-MS, Thermo Fisher Neptune Plus) at the Institute of Environmental Physics (IUP), Heidelberg University, Germany. For age calculations the half-lives of ^{234}U and ^{230}Th published in Cheng et al. (2013) were used. The mass spectrometry setup and data treatment follows the methods recently updated in great detail by Kerber et al. (2023). We used the initial δ^{234}U value and ^{232}Th contamination to evaluate the quality of the ^{230}Th/U ages. The ^{232}Th concentration is directly related to deposition of Th from seawater or non-carbonate material and induces an increase in ^{230}Th, that is, age correction and increasing uncertainty when propagating correction errors. Here, solely corals with a ^{232}Th content below 3.6ng were selected. The initial ^{230}Th correction is, thus, negligible when applying an upper thermocline seawater ^{230}Th/^{232}Th ratio of 8 ± 4. To test the U series closed system presumption, we assume that all corals must have an initial ^{234}U/^{238}U ratio (δ^{234}U$_{initial}$) of ±7‰ of the modern ocean δ^{234}U$_{sw}$ (146.8‰) (Andersen et al., 2010; Reimer et al., 2009). The selected range of δ^{234}U$_{sw}$ variability of ±7‰ includes the known glacial reduction in seawater δ^{234}U by some −5‰ ± 2‰ (Chutcharavan et al., 2018). Due to differences in the use of isotope standards, seawater values can differ by about ∼1.2‰ between laboratories and publications. Kipp and Tissot (2022) recently reassessed δ^{234}U$_{sw}$ to 145.55‰ ± 0.28‰ using a normalization of the data to the CRM 112A certified value, whereas we measure a value of CRM 112A (also known as SRM 960) which is 1.2‰ higher. We use the seawater value of 146.8‰ (Andersen et al., 2010) to be self-consistent with our normalization approach to HU1 standard, which we presume in secular equilibrium (Wefing et al., 2017). Such difference in normalization does not impact the absolute ages as those are always normalized to a presumed secular equilibrium value using the half-lives of Cheng et al. (2013). The entire data set is available at PANGAEA. ^{230}Th/U ages are reported referenced to 1950 AD (years BP).

2.3. Radiocarbon Dating

Approximately 15–20 mg of sample material from the previously thoroughly mechanically cleaned coral fragments was leached in hydrochloric acid (4% HCl) for about 30 s and dried afterwards. Extraction and graphitization were carried out at the IUP, Heidelberg University, Germany, according to Therre et al. (2021). The iron-graphite mixture was measured on an accelerator mass spectrometer (AMS, MICADAS) at the Curt-Engelhorn Center for Archeometry in Mannheim, Germany (Kromer et al., 2013; Synal et al., 2007). The blanks obtained from marble and IAEA-C1 standard showed ^{14}C ages >50,000 years (Therre et al., 2021). To evaluate the quality and reproducibility of the ^{14}C measurements, 13 duplicate samples were prepared and measured in addition to 13 IAEA-C2 standards. All duplicates agree within the 2σ range, ∼85% within 1σ. For the IAEA-C2 standard, a mean age of (7,125 ± 12) a (literature: (7,135 ± 6) a) showed an improvement over previous measurements (see Therre et al., 2021). To present our data, we calculated Δ^{14}C (known-age radiocarbon correction): Δ^{14}C$_{coral}$=(Fm×$e^{(\text{calendar age}/8267)}$ − 1) × 1,000 (Stuiver & Polach, 1977). Since this value is best used in combination with the reconstructed ^{14}C content of the atmosphere, we calculated the offset $\Delta\Delta^{14}$C as Δ^{14}C$_{coral}$ − Δ^{14}C$_{atmosphere}$ and the Benthic-Atmosphere (B_{atm}) age as ^{14}C$_{age, coral}$ − ^{14}C$_{age, atmosphere}$ to account for the varying atmospheric ^{14}C inventory (Chen et al., 2015). We used IntCal20 (Reimer et al., 2020) and SHCal20 (Hogg et al., 2020) as atmospheric references. All previously published ^{14}C data presented here were recalculated according to the updated atmospheric calibration curves. Detailed information about the uncertainty ellipses using a Monte-Carlo approach can be found in Ruckelshausen (2013). The Python codes are freely available upon request. Even after rigorous quality control, four of the 122 fossil corals had to be excluded from the results

and discussion, because they showed $\Delta^{14}C$ values above the IntCal20 reconstruction (seawater ^{14}C > atmospheric ^{14}C). The entire data set is available at PANGAEA.

2.4. Modeling Radiocarbon

We compared our observations with the simulation results of three numerical simulations obtained from an enhanced version of the Large Scale Geostrophic Ocean General Circulation Model (LSG, Maier-Reimer et al. (1993), for the enhancements see Butzin et al. (2005), and further references therein). The model has a horizontal resolution of 3.5° and a vertical resolution of 22 unevenly spaced levels. Radiocarbon is simulated as $\Delta^{14}C$ following Toggweiler et al. (1989). The oceanic uptake of ^{14}C is calculated according to Sweeney et al. (2007), using atmospheric CO_2 values (Köhler et al., 2017) and concentrations of dissolved inorganic carbon in surface water simulated by Hesse et al. (2011). The LSG model is forced with monthly fields of recent and glacial wind stress, surface air temperature, and freshwater flux derived in previous climate simulations (Lohmann & Lorenz, 2000; Prange et al., 2004). To capture the range of past ocean-climate variability and its impact on marine ^{14}C records, we considered three climate forcing scenarios which are discussed in detail by Butzin et al. (2005). In summary, one scenario (PD) employs present-day climate background conditions approximating the Holocene and interstadials. Another scenario (GS) aims at representing the LGM and features a shallower AMOC than scenario PD weakened by about 30%. The third climate scenario (CS) mimics cold stadials with further AMOC weakening by about 60% compared to PD. Scenarios PD and CS typically represent the lower and upper bounds of marine ^{14}C depletion with respect to the contemporaneous atmosphere ($\Delta\Delta^{14}C$). The simulations were run with transient values of atmospheric $\Delta^{14}C$ (Reimer et al., 2020) and evaluated at the model coordinates nearest to the CWC sites.

3. Results

3.1. ^{230}Th/U Dating

Overall, U concentrations are within the typical range of 2.5–5.5 μg/g. Median ^{232}Th concentrations are 0.5 ng/g due to the strict selection criteria, and median $\delta^{234}U$ values are 146.3‰, identical within uncertainty to the expected modern seawater value. Note that $\delta^{234}U$ clearly shows the known systematic deviation from constant $\delta^{234}U$ values during the last glacial for corals from Mauretania and Angola, while observations from the AFC and Alboran Sea reveal punctuated and even systematic higher values in agreement with the northern source of excess ^{234}U derived by Chen et al. (2016). In conclusion, we assume all ^{230}Th/U ages are reliable and that the initial $\delta^{234}U$ isotopic composition reflects past seawater. The ages used for radiocarbon reconstruction range from 31.56 ka to 52 years. The distribution of ages is different for each site. For the Alboran Sea, coral ages are only available for the end of the deglaciation from 14.73 to 9.65 ka. For AFC, we obtain ages from 21.1 ka to 52 years, reflecting the LGM, termination 1, and the Holocene. At Mauritania, ages range from 25.5 to 12.5 ka, representing the LGM as well as the Bølling-Allerød (B/A) and Younger Dryas (YD). Most of the results were obtained from Angola, where corals provide ages from 31.6 ka to 41 years. Consequently, Angola provides observations from the last glacial and LGM to the present.

3.2. Radiocarbon Dating

In general, our $\Delta^{14}C$ values follow the atmospheric trend with $\Delta^{14}C$ values decreasing from 400‰ to −65‰ over the past 32 ka (Figure 2a; IntCal20, Reimer et al., 2020).

Alboran Sea corals confirm previous results (McCulloch et al., 2010; Figure S1 in Supporting Information S1), showing overall well-ventilated water with an average $\Delta\Delta^{14}C$ value of −55‰ ± 34‰ and B_{atm} age of 400 ± 230 years. Two values are strongly depleted with $\Delta\Delta^{14}C$ of −140‰ and −130‰, corresponding to a doubling of B_{atm} ages from 450 to 900 years at 12.4 ± 0.04 ka and at 13.6 ± 0.2 ka. The second depletion coincides with the YD cold reversal. A comparison with numerical simulations is not possible here, since the Alboran Sea is not represented in the LSG Ocean General Circulation model.

AFC reveal well-ventilated water with an average $\Delta\Delta^{14}C$ of −66‰ ± 30‰ and B_{atm} age of 450 ± 170 years since the LGM. The mean $\Delta\Delta^{14}C$ value is thus ~10‰ lower compared to the one of the Alboran Sea, but identical within uncertainty (Figure 2b). Over the last 14 ka, the results agree within uncertainty with the upper bound of
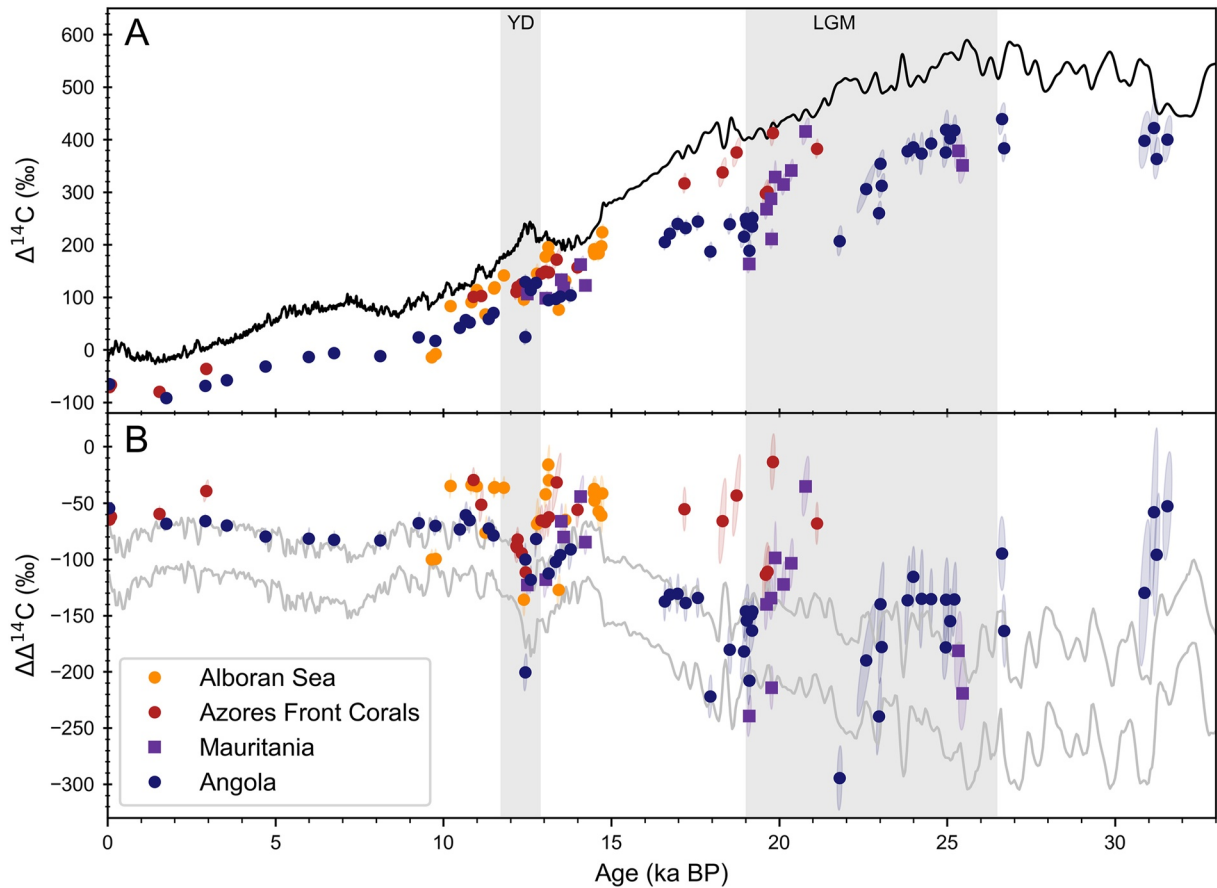
Figure 2. Radiocarbon variability of the east Atlantic thermocline obtained from cold-water corals (CWC) in this study. (a) $\Delta^{14}C$ with IntCal20 as atmospheric reference (black line, Reimer et al., 2020). (b) $\Delta\Delta^{14}C$ evolution ($\Delta^{14}C$ offset between ocean and atmosphere), including upper and lower bounds of the LSG model simulation results off Angola (gray lines). Error ellipses represent the 2σ uncertainty. Angola basin CWC results are mostly at the upper bound of the simulation. The ^{14}C values of the Northern Hemisphere remain well-ventilated, in sharp contrast to the corresponding simulation results (Figures S2 and S3 in Supporting Information S1). Differences between south and northeast Atlantic vanish with the onset of the Younger Dryas.

the numerical simulation, which corresponds to the lowest B_{atm} ages (Figure S2 in Supporting Information S1). In contrast, for the LGM and beginning deglaciation, the numerical simulation yields $\Delta\Delta^{14}C$ of $-120‰$, while the observations are on average $-70‰$ (Figure S2 in Supporting Information S1). Only at 19.6 ka do model and observations agree, with two individual observations of $-110‰$, again corresponding to the upper bound of the model output. Prior to the YD, from 14 to 12.9 ka, our results reveal low B_{atm} ages of 220–460 years. During the YD, the observations confirm a 250 year long decrease in ventilation, followed by an increase in ventilation at 11.5 ka to modern values. Our AFC results support previously documented synchronous B_{atm} age excursions reconstructed at significantly deeper depth west of the New England Seamounts (NESM) (Eltgroth et al., 2006; Robinson et al., 2005).

Between 25 and 12.5 ka, the corals off Mauritania show $\Delta\Delta^{14}C$ values with a mean of $-125‰ \pm 60‰$, corresponding to a mean B_{atm} age of 770 years. Therefore, the CWCs from Mauritania report water masses that are on average 320 years older than the more northerly sites. However, within the overall high variability of B_{atm} ages from 1,500 to 300 years, the ventilation is partially identical to the northern sites as well as the southern sites (see below). If compared to the LSG model, the observations at 14 to 12.5 ka and at 25.3 to 25.4 ka are in perfect agreement with the simulation, while the observed $\Delta\Delta^{14}C$ values around the LGM and the onset of deglaciation are initially higher by up to $70‰$ (21 ka) and then lower by up to $50‰$ (19 ka) (Figure S3 in Supporting Information S1).

The overall most important data set is generated for Angola. Here, we reconstruct well-ventilated waters around 31 ka and from 13.8 ka (Figure 2 and Figure S4 in Supporting Information S1), with a mean $\Delta\Delta^{14}C$ of -80 ± 17

and B_{atm} age of 580 ± 120 years. In between, $\Delta\Delta^{14}C$ values and B_{atm} ages are highly variable, showing lowest values of $-295‰$ (1,700 years B_{atm} age) at 21.8 ka. In contrast to the results of the northern sites, the radiocarbon record from Angola is mainly at the upper bound of the LSG model results. We note that the model does not resolve the Angola gyre circulation and therefore cannot correctly simulate the associated upwelling in this region. Nonetheless, 92% of the data are captured by the range of $\Delta\Delta^{14}C$ values simulated by the LSG model. Solely at 31 ka do the observations systematically exceed the model results (Figure S4 in Supporting Information S1). The record reveals several periods of centennial variations from 50‰ to 100‰ (250–500 years B_{atm} age), with only the last two within model uncertainty (19 and 23 ka). The LSG model simulates a gradual increase of ventilation between 18 and 14 ka, which is confirmed in terms of measured values. It is important to note that the B_{atm} ages prior to the simulated ventilation increase show high B_{atm} ages and large scatter with an average value of $1,060 \pm 180$ years between 19.2 and 17.9 ka, followed by a 980 year long period of moderately higher but extremely constant B_{atm} ages averaging 840 ± 30 years during the simulated increase between 17.5 and 16.6 ka. Between 16.6 and 13.8 ka, the water off Angola reduced the age by another 130 years to an average of 650 ± 25 years from 13.8 to 13.5 ka. This ventilation trend was interrupted during the Antarctic Cold Reversal (ACR) some 13.5 to 13.1 ka ago, when B_{atm} ages increased again by 100 ± 50 years, as simulated. Subsequently, a decrease in ventilation is recorded during the YD period until, finally the well-ventilated (quasi modern) state during the Holocene is reached.

The observed radiocarbon ages off Angola are broadly consistent with observations in the equatorial Atlantic at 750–1,492 m depth (Chen et al., 2015, 2020), southwest Australia at 675–1,788 m depth (Trotter et al., 2022), and south of Tasmania at 1,430–1,950 m depth (Hines et al., 2015) (Figure 3c). These deeper and more distant sites show identical values within uncertainty or moderately higher B_{atm} ages. At 21.8 ka, the B_{atm} age at Angola increased to a similar high value as observed off southwest Australia (Figure 3c).

Lastly, a remark on the B/A and YD period of Northern Hemisphere warming some 14.9 ka and 12.5 ka ago. The northern and southern Atlantic records deviate by ∼250 ± 50 years (B_{atm} age, Figure 4c). With the onset of the YD at 12.5 ka, the ^{14}C gradient between the North and South Atlantic ultimately vanished. The YD resolves a pronounced $\Delta^{14}C$ decline of ∼80‰ within 1,000 years at all sites (Figure 2b).

4. Discussion

The above presented results fill out an important data gap in the recent compilation by Skinner and Bard (2022). Corals from Angola and Mauritania enable us to investigate the southern extent of the well-ventilated water, as well as the northern and vertical extent of aged, southern-sourced water. Thus, we focus on the upper branch of the Atlantic circulation and its horizontal fronts. The physical nearness of our corals to oceanic fronts makes them sensitive to water mass changes, particularly the intrusion of older, southern sourced or underlying water. AFC shed light on the important role of the AF in the North Atlantic. In general, low mixing is thought to have occurred between the two circulation cells during the LGM (Adkins, 2013; Lund et al., 2011), with a boundary at roughly 2,000–2,500 m depth (Rafter et al., 2022), thus well below the coral sites. In the following discussion we will focus on several key observations. We first examine the overall Atlantic thermocline ventilation since 32 ka. Subsequently, we investigate the well-ventilated state in the North Atlantic during the LGM. Corals from Angola show striking similarities to previous radiocarbon records, hence the South Atlantic connectivity and its northern limit are explored. Finally, the first insights into thermocline ventilation during the B/A warm period, the ACR, and YD provided by our records are discussed in detail.

4.1. The Atlantic Thermocline Ventilation Since 32 ka

Here, we define the thermocline as the interface between the well-mixed surface layer and the underlying colder water at intermediate depths between 200 and 1,000 m. Note that the physical thermocline, as the region of downward temperature drop, can extend to 2,000 m in the Atlantic. The upper part of the ocean at mid-depth discussed here is closely related to the dynamics in the surface ocean, as it is the host of strong eddy driven re-circulation gyres, mid-depth boundary currents and specific intermediate water masses (such as MOW and AAIW). Moreover, this depth interval is influenced by the presence of oceanic fronts, such as the AF, CVFZ, and the ABF, which locally cause horizontal water mass gradients and/or vertical exchanges. Overall, this part of the ocean is today generally influenced by recent ^{14}C changes in the atmosphere, that is, bomb ^{14}C. Consequently,
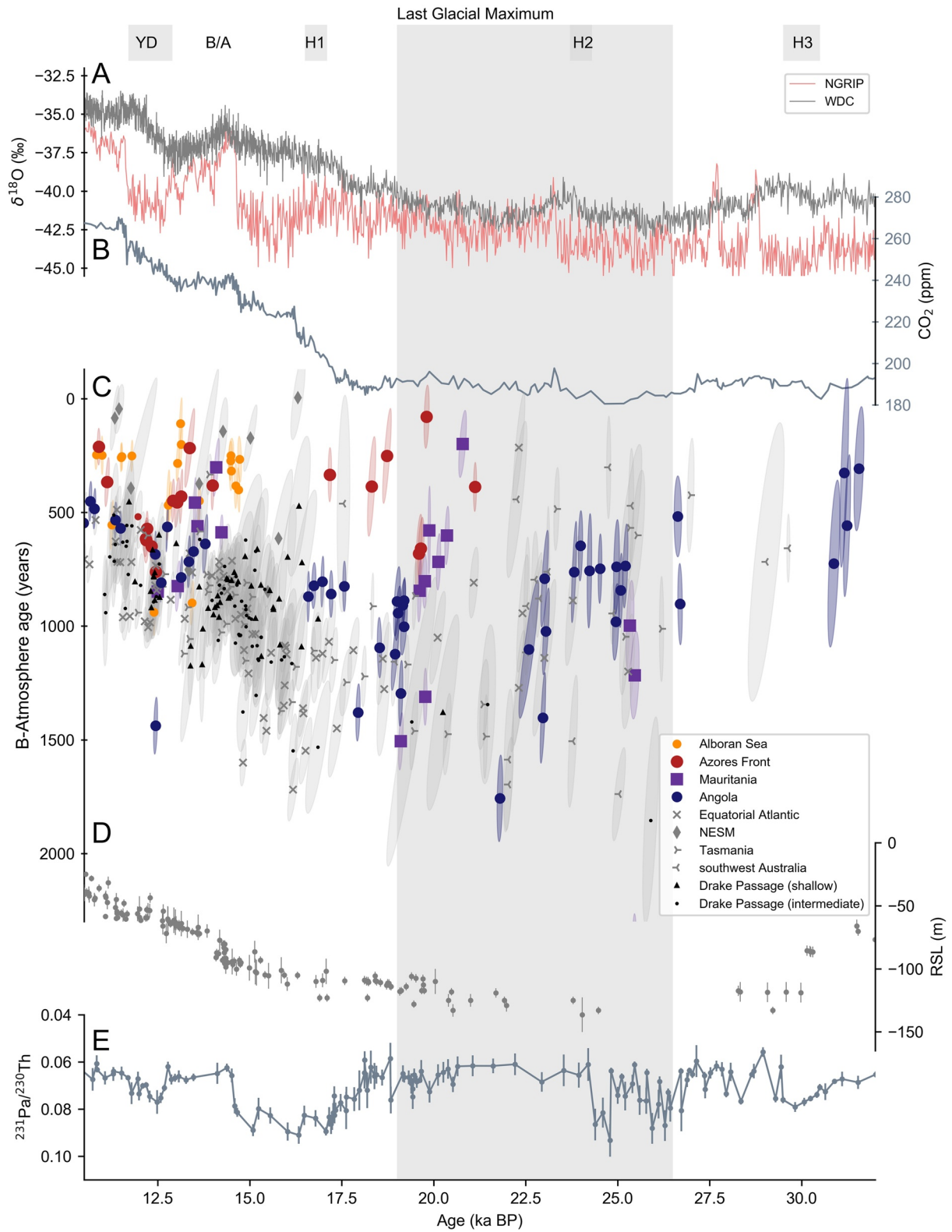
Figure 3.

the apparent age of all these water masses must be less than 60 years (Figure 1b). Assuming an average reservoir effect of 380 years (Heaton et al., 2020) of the modern Atlantic (neglecting regional variability), the radiocarbon age of these water masses would be expected in the order of 440 years. The reason for the good ventilation state of these water masses is their close connection to the surface via turbulent seasonal mixing, wind driven upwelling and downwelling, and shallow overturning of intermediate waters in subpolar and subtropical regions (Skinner & Bard, 2022).

In fact, all studied sites reveal similarly young B_{atm} ages since the YD and in various regions prior to it. In particular, AFC show persistently such well-ventilated waters, as reflected in the median B_{atm} age (450 ± 170 years), whereas further south such low B_{atm} ages occur only at 31 ka (Angola), 20 ka (Mauritania) and the B/A. Consequently, during most of the glacial period between 26.8 to 16.5 ka, the thermocline south of the modern AF aged 330–440 years, as indicated by the difference between the expected modern age (440 years) and the median observed age (770 and 880 years). In addition, the median B_{atm} age reveals a moderate north-south gradient of 110 years, while a similar ventilation age difference exists between AFC and Angola since the B/A. Therefore, the glacial intermediate depth age gradient per latitude was enhanced.

4.2. North Atlantic Ventilation During the LGM

The ^{14}C reconstructions of the AFC are within the transition zone between subtropical and subpolar North Atlantic thermocline waters (located around the Azores and Great Meteor Seamount, 800–1,000 m depth). Within uncertainty, the AFC are in accordance with ventilation ages off Mauritania at ∼560–590 m depth, ranging from 80 to 680 years between 20 and 21 ka (Figure 3c). The mean age of ∼500 years is close to the common pre-bomb surface reservoir age of 380 years, demonstrating the strong surface to thermocline ocean connectivity. Today, the presence of well-ventilated thermocline waters within this region is caused by the regional downwelling of carbon due to Ekman pumping, the injection of well-ventilated MOW and shallow convection in the Labrador Sea as part of the subpolar gyre. These processes permit a fast overturning of carbon as detected today in the decadal turnover of bomb-radiocarbon and other ventilation tracers (GLODAPv2.2) and must have operated at all times north of the AF to sustain the high degree of ventilation throughout the last glacial and even deglaciation. The strong resemblance of B_{atm} ages near the glacial AF and CFVZ (Mauritania) argues for basin scale recirculation of well-ventilated water north of the wind-driven front separating southern and northern sourced waters. In addition, this observation suggests a southward shift of the AF, to remove the difference in B_{atm} ages between south and north of the modern AF. The abundance of specific planktic foraminifers as an indicator for the presence of the AF during glacial times supports this view (Reißig et al., 2019; Schiebel et al., 2002).

Strikingly, Mauritania CWCs not only show similarities with AFC, but also punctually match the radiocarbon signal observed in corals further south at 19.7 and 19.1 ka (equatorial Atlantic and Angola, Figure 3c). Previous studies suggested a southward displacement of the CVFZ during the LGM (Huang et al., 2012; Wienberg et al., 2018), which would lead to an influence of northern-sourced water near Mauritania, in contrast to the southern-sourced water bathing the corals today. This is consistent with the well-ventilated signal, with reconstructed B_{atm} ages < 1,000 years, matching the AFC and the predicted pattern by Skinner and Bard (2022) (Figure S6 in Supporting Information S1). However, the episodic resemblance with southern coral B_{atm} ages (>1,000 years) argues for multiple shifts of the CVFZ, causing punctually drastic decreases in ventilation through the advance of older southern water. Between 19.7 and 19.1 ka (Figure 2c), two Mauritanian corals show strong B_{atm} age increases, which are likely caused by latitudinal movements of the CVFZ, such that the subtropical and subpolar North Atlantic thermocline was located between well and poorly ventilated waters. In addition to the horizontal frontal movement, a severe contrast between the well-ventilated water of the northern thermocline and the strongly aged water below the thermocline results in a high sensitivity to vertical fluctuations. However, we have yet no possibility to resolve the depth profile and thus cannot distinguish from the few age measurements, whether horizontal or vertical changes caused the two elevated reservoir ages.

Figure 3. Radiocarbon age variability and climate change between 10 and 32 ka. (a) $\delta^{18}O$ records of NGRIP, Greenland (Bazin et al., 2013) and WDC, Antarctica (WAIS, 2015). (b) CO_2 compilation record (Bereiter et al., 2015). (c) B-Atmosphere age reconstructed from cold-water corals: Azores Front Corals, Mauritania, and Angola (this study), as well as equatorial Atlantic (Chen et al., 2015, 2020), New England Seamounts in 1,100–1,400 m depth (NESM; Eltgroth et al., 2006; Hines et al., 2019; Robinson et al., 2005; Thiagarajan et al., 2014), Tasmania (Hines et al., 2015), southwest Australia (Trotter et al., 2022) and Drake Passage (DP, Burke & Robinson, 2012; Chen et al., 2015; Li et al., 2020). Note: All B_{atm} ages have been recalculated using IntCal20 and SHCal20 (Hogg et al., 2020; Reimer et al., 2020). DP sections after (Li et al., 2020), depending on the location and depth of the corals. (d) Observed relative sea level (Lambeck et al., 2014). (e) $^{231}Pa/^{230}Th$ records of sediments from the Bermuda rise (Böhm et al., 2015; Lippold et al., 2019; McManus et al., 2004).
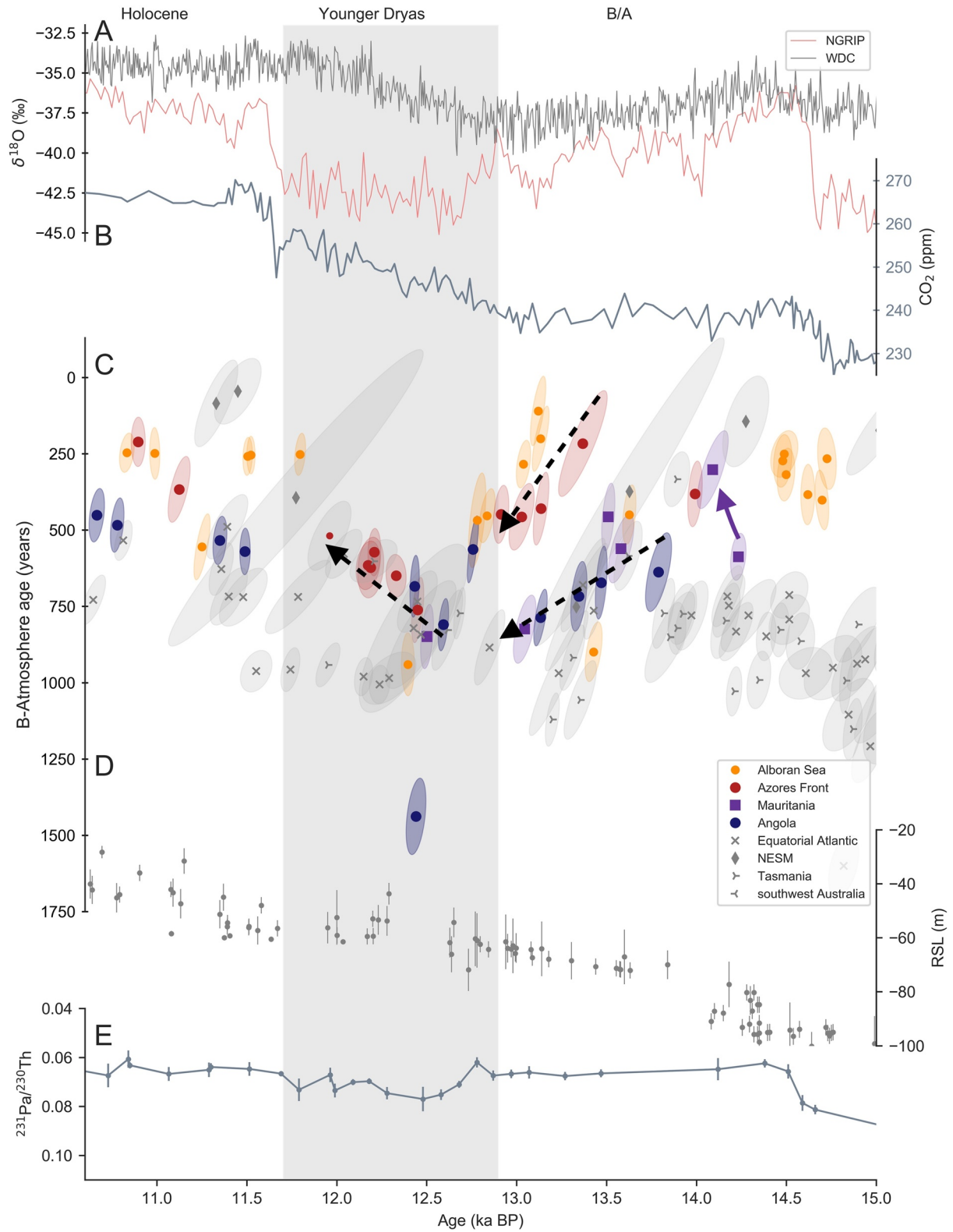
Figure 4.

This ^{14}C pattern of the wind-driven subsurface circulation is not captured by the LSG model (Figures S2 and S3 in Supporting Information S1), which systematically underestimates $\Delta\Delta^{14}C$ in the northeastern subtropical Atlantic prior to the B/A, except for the highest B_{atm} ages and respective lowest $\Delta\Delta^{14}C$ values obtained in AFC. Nevertheless, the model reveals a higher degree of ventilation if compared to the two exceptional poorly ventilated corals off Mauritania. Therefore, the model simulates a moderately lower ventilation state for the northeast Atlantic, but certainly does not infer a wind driven frontal zone. This observation is, however, not surprising as the wind driven fronts would certainly require a higher physical resolution of the LSG model. Also processes such as coastal upwelling are not implemented.

Regarding the origin of the well-ventilated thermocline waters, several studies suggest a shallow, well-ventilated water mass during the LGM (e.g., Chen et al., 2015; Cléroux et al., 2011; Curry & Oppo, 2005; Freeman et al., 2016; Keigwin, 2004; Slowey & Curry, 1992), which may be Glacial North Atlantic Intermediate Water formed in the western part of the North Atlantic (Lynch-Stieglitz et al., 2007). However, we note that our samples are too shallow to represent this water mass.

The comparably low B_{atm} ages observed here seem to trace this water mass from west to east along the AF even down to Mauritania, implying a persistent strong connection of mid-depth circulation and westerly winds. Alternatively, MOW would provide a source of well-ventilated water from the east. However, this is not consistent with the finding of an eastern basin advance of AAIW (Dubois-Dauphin et al., 2016). Therefore, we favor the hypothesis of a vigorous ventilation by North Atlantic subpolar waters recirculating north of the glacial AF. However, the exact position of the front and the predominant mixing processes remain elusive.

4.3. The South Atlantic Connectivity and Its Northern Limit During the Last Glacial

While our South Atlantic upper thermocline ^{14}C record (Angola) shows well-ventilated thermocline waters during the Holocene, a different picture emerges during the LGM. Apparently, at 31 ka aged waters replaced the well-ventilated water off the coast of Angola. The clear aging of thermocline water and amplified glacial age depth gradients compared to today (Skinner & Bard, 2022) may reflect a combination of numerous processes, which, however, influence all southern oceans. Such processes are increasing sea ice cover in south polar regions inhibiting gas exchange and thus ventilation, and/or overall reduced ventilation of the deep oceans (AMOC weakening), and/or increased storage of respired CO_2 in the deepest layers and upward mixing into the thermocline ocean (Skinner & Bard, 2022). In the deep ocean, glacial haline stratification is thought to decrease vertical mixing across water masses as compared to the thermohaline stratification today, leading to more stratification (Adkins, 2013). Aged Glacial Pacific Deep Water can invade the deep South Atlantic through the Drake Passage (DP) (Howe et al., 2016; Williams et al., 2021; Yu et al., 2020). Simultaneously, a reduced Agulhas leakage occurs (Franzese et al., 2006), limiting the influence of the Indian Ocean on the southern Atlantic. During the LGM, an enhancement of the Antarctic Circumpolar Current (ACC) increased eastward transport mainly in the intermediate water layers through the DP (Clauzet et al., 2007). This strengthened the intermediate layer exchange between the Pacific and the South Atlantic, as well as with the Indian Ocean, and would thus cause similar ventilation conditions in far distant regions across the deep Southern Oceans. Additionally, the Tasman Sea could have played an important role in the interoceanic exchange of intermediate water masses (Struve et al., 2022). The combination of all these processes would lead to a strong Southern Ocean connectivity, but also far higher sensitivity to differently aged water masses.

CWCs located in the DP recorded radiocarbon depleted waters during the last glacial period (Figure 3c and Figure S5 in Supporting Information S1) (Burke & Robinson, 2012; Chen et al., 2015; Li et al., 2020), and model results suggest a South Atlantic thermocline dominated by water originating from the DP (Paul & Schäfer-Neth, 2003), likely penetrating to at least 800 m depth at the equator (Clauzet et al., 2007). Indeed, we observe B_{atm} ages off Angola at 259–457 m depth, which are identical to previously recorded ages from the equatorial Atlantic at 795–845 m depth (Chen et al., 2015; Figure 3c). Furthermore, B_{atm} ages at Angola are similar to those observed

Figure 4. Radiocarbon age variability during the Termination, 15–11 ka BP. (a) $\delta^{18}O$ record of NGRIP, Greenland (Bazin et al., 2013) and WDC, Antarctica (WAIS, 2015). (b) CO_2 compilation record (Bereiter et al., 2015). (c) B-Atmosphere age reconstructed from cold-water corals from the Alboran Sea (this study), Azores Front (this study and Eltgroth et al. (2006)), Mauritania (this study), Angola (this study), New England Seamounts in 1,100–1,400 m depth (NESM; (Eltgroth et al., 2006; Hines et al., 2019; Robinson et al., 2005; Thiagarajan et al., 2014)) and equatorial Atlantic (Chen et al., 2015, 2020). Northern and southern thermocline water differ by ~250 ± 50 years, they join with the onset of the Younger Dryas (YD). (d) Observed relative sea level, (Lambeck et al., 2014). (e) $^{231}Pa/^{230}Th$ records of sediments from the Bermuda rise (gray line, Böhm et al., 2015; Lippold et al., 2019; McManus et al., 2004). The gray bar indicates the duration of the YD.

in far distant locations from the Southern Ocean, that is, Tasmania and southwest Australia. Given the prominent similarities between records from Angola, southwest Australia (Trotter et al., 2022) and Tasmania (Hines et al., 2015), as well as the equatorial Atlantic (Chen et al., 2015) and parts of the DP (Burke & Robinson, 2012; Chen et al., 2015; Li et al., 2020), our new $\Delta^{14}C$ data from CWCs off Angola strengthens the evidence of intermediate water connectivity and ventilation of the thermocline across the South Atlantic up until the equatorial Atlantic and large parts of the Southern Ocean.

The shallow depth of the corals off Angola and its radiocarbon similarity with deeper and far distant sites implies an influence of interior advective patterns. Those connect in the mid-depth southern and equatorial Atlantic and fuel ^{14}C depleted waters below the wind driven surface ocean. As a consequence, aged water distributed by the ACC must be transported by currents over a wide depth range during the LGM. Remarkably, high temporal variability of the ^{14}C signal, expressed as abrupt shifts in B_{atm} age between 240 and 600 years magnitude, are recorded simultaneously by CWCs off Angola (259–457 m depth) and in the Southern Ocean (675–1,950 m depth) (Hines et al., 2015; Trotter et al., 2022) at 26.6, 25, 23, and 19 ka. These observations indicate short periods of injection of very old, likely deep water into the thermocline, causing a dynamic radiocarbon range within the mid-depth circulation patterns. This coherence of multiple independent time-series strengthens the hypothesis of advective connectivity (Skinner & Bard, 2022). The close connection of thermocline and surface ocean highlights the importance to consider ventilation age variability in marine radiocarbon age calibrations for the Southern Oceans.

During deglaciation, the southern connectivity, expressed in the similarity of the ^{14}C signals, seems to continue (Figure 3c), until the Angola record shows moderately lower B_{atm} ages of ~830 years at 17.6 ka compared to the equatorial Atlantic, Tasmania, and DP. Since advection from well-ventilated water from the north can be ruled out due to the lower ventilation signal near the equator, this sudden increase in ventilation off Angola must be related to downward mixing of carbon from the surface ocean. It coincides with AMOC weakening indicated by $^{231}Pa/^{230}Th$ (Figure 3e), and it is simultaneous to a change in intermediate and circumpolar circulation regimes across the Indo-Australian Southern Ocean (Trotter et al., 2022). Moreover, atmospheric CO_2 concentrations increased by 20 ppm (Figure 3b; Bereiter et al., 2015). In addition, these changes coincide with an Antarctic Sea-Ice Retreat (WAIS, 2013), rising sea-level (Lambeck et al., 2014) (Figure 3d), and Southern Hemisphere warming (e.g., WAIS 2015; Figure 3a). Accordingly, at least since 17.6 ka BP, the upper southern Atlantic thermocline has been less influenced by old, deeper water masses from the south and has likely contributed to the increase in atmospheric CO_2 through the transfer of respired carbon. Overall, the Angola corals provide a strong connectivity to all other thermocline to mid-depth ocean sites studied so far, with Angola thermocline water ages constituting the "young" envelop of the strong age depth gradients. The observed variability reflects the expected larger depth gradients and dynamics during the last glacial.

4.4. The Bølling-Allerød, Antarctic Cold Reversal and Younger Dryas

With the start of the B/A warm period and the subsequent ACR, all thermocline water sites investigated here show strong ventilation (Figure 4c), which reflects the increase in AMOC toward its modern state. In addition, CO_2 increased by 50 ppm, and most of the global warming and a significant sea-level rise were achieved (Figure 3). Accordingly, old carbon previously stored in the Southern Hemisphere oceans at depths of 250–1,500 m was rejuvenated. The deglacial ventilation caused the high variability of the last glacial to vanish and lead to a decrease of average B_{atm} ages between 800 and 1,500 years to values <700 years, which were already similar to modern ages.

Previous studies showed evidence of a ventilation anomaly during the B/A and ACR (e.g., Barker et al., 2010; Chen et al., 2015; Li et al., 2020; Robinson et al., 2005; Skinner et al., 2021), characterized by well-ventilated deep and mid-depth water throughout the entire Atlantic, with a maximum B_{atm} ages of 1,000–1,500 years (Rafter et al., 2022). Note that the LGM represented a time with B_{atm} age of up to ~2,500 years in the deep Atlantic (Rafter et al., 2022; Skinner & Bard, 2022). The B/A represents a warm period in the Northern Hemisphere, while the ACR describes a synchronous cooling of the Southern Hemisphere. During this time, both atmospheric CO_2 (Marcott et al., 2014) and $\Delta^{14}C_{atm}$ (Hogg et al., 2020; Reimer et al., 2020) remained constant, possibly marking the end of the massive outgassing of respired carbon from the deep ocean at 16.3 ka, which was proposed previously (Marcott et al., 2014). The new ^{14}C results provide further evidence of the complex ventilation history of the Atlantic, giving first insights into thermocline ventilation during the millennial climate variability of the B/A, ACR and the following Northern Hemisphere cold reversal of the YD period. An enhancement of ventilation during the B/A and ACR was previously suggested for the

deep and lower intermediate North Atlantic (900–2,000 m depth) through the reconstruction of ^{14}C using foraminifera and CWCs (Skinner and Bard 2022, and references therein). The new findings are clearly in line with these earlier suggestions of enhanced Atlantic ventilation during the B/A and ACR, most likely caused by significant deepening of the AMOC (Barker et al., 2010). Between 14.5 and 11 ka, ventilation ages in the equatorial and South Atlantic thermoclines overall decreased from 1,000 to 450 years (Figure 4c). However, the intensified ventilation paused at 13.8 ka, leading to a re-aging of thermocline water masses until the start of the YD.

In contrast to this southern behavior, ^{14}C records near the AF and within the Alboran Sea reveal an even more complex pattern within their overall well-ventilated state (B_{atm} ages between 220 and 450 years on average). Assuming a strong teleconnection between these locations via the spreading of MOW and Ekman pumping near the AF, we propose a combined view of those two northern records. B_{atm} ages differed between waters north and south of the AF by ∼250 ± 50 years between 13.5 and 13 ka (Figure 4c). The AF ventilation state decreased from 250 to 750 years between ∼13.4 and 12.5 ka, while South Atlantic records decreased from 500 to 850 years between ∼13.6 and 13 ka. We observe an abrupt interruption of the general AF aging trend with sudden aging of Alboran Sea water at 13.6 ± 0.2 ka. This implies a northward shift of the AF, allowing aged water of southern origin to penetrate more efficiently into the thermocline of the North Atlantic and thus into the Mediterranean Sea. Since the position of the AF is presently north of the position expected for colder climates, periods of merged Southern Hemisphere and North Atlantic B_{atm} ages likely reflect enhanced northward salt exports required to trigger deep convection. This implies possibly multiple launches and failures of the AMOC, which are not yet visible in the sparse temporal resolution of ^{231}Pa/^{230}Th records (Figure 4e).

Regarding CWCs from Mauritania, observed rapid radiocarbon fluctuations at the beginning of the B/A period must be related to the position of the CVFZ. Nowadays the sites are under the influence of southern sourced water. At 14.2 ka, Mauritania shows a poorly ventilated radiocarbon signal, which we assume to reflect a southern source as well. In the following hundred years, the signal switches to better ventilation and thus most likely a northern source (14.1 ka), consistent with corals from the AF and NESM, and clearly distinct to the equatorial Atlantic (Figure 4c). This observation confirms previous studies, describing a sudden southward displacement of the CVFZ during the B/A (Huang et al., 2012; Romero et al., 2008; Wienberg et al., 2018). This frontal displacement was, however, not permanent. It coincides with the Older Dryas, during which weakening of the AMOC was suggested (Stanford et al., 2006; Thornalley et al., 2011), which has been linked to changes in freshwater input and routing into the ocean (review by Carlson and Clark (2012) and references therein). Following the series of events, the Mauritania ventilation signal returned to the southern less ventilated signal, which prevails until present. This indicates an alternating water mass influence off Mauritania during the Northern Hemisphere warming and ice sheet decay, and thus multiple displacements of both the AF and CVFZ across the B/A and YD.

With the onset of the YD at 12.5 ka, the ^{14}C gradient between the North and South Atlantic finally vanished, and homogenous radiocarbon ages were established of the intermediate waters from the NESM in the west to the equatorial Atlantic (Chen et al., 2015, 2020; Eltgroth et al., 2006; Robinson et al., 2005) and the intermediate waters of the AF (this study and Eltgroth et al. (2006)), Mauritania, and partially Angola (this study). Previous observations have inferred decreased ventilation during the YD (e.g., Chen et al., 2015; Eltgroth et al., 2006; Robinson et al., 2005; Schröder-Ritzrau et al., 2003; Skinner & Shackleton, 2004; Skinner et al., 2014, 2021; Waelbroeck et al., 2001), consistent with a collapse of the AMOC and a reduction in North Atlantic Deep Water export, as seen in the ^{231}Pa/^{230}Th record (McManus et al., 2004; Figure 4e). Our new results advocate that the aging of the North Atlantic is significantly stronger and in situ compared to the southern Atlantic when excluding one exceptionally low ^{14}C value at 12.45 ka, recording a signal even older than CWCs from the DP (Burke & Robinson, 2012; Chen et al., 2015; Li et al., 2020, Figure S5 in Supporting Information S1). This one exceptional value off Angola is, however, consistent with ^{14}C dating on benthic foraminifera from the Brazil margin (Skinner et al., 2021, Figure S6 in Supporting Information S1). Thus, it remains unclear whether this value can be excluded or whether it indicates a sudden aging of the subtropical South Atlantic thermocline, which could also be caused by frontal movement. The combination of all available records suggests that deep convection was interrupted for 300–500 years between 12.8 and 12.4 ka (Figure 4c). We emphasize that the full rejuvenation of the subtropical thermocline waters north and south of the equator was achieved during the YD but not only after the event.

Note that sea-level was still some 60 m below present (Lambeck et al., 2014; Figure 4d). This implies that the size of the residual Northern Hemisphere ice sheets was still vast, when modern type ventilation patterns have been ultimately established.

5. Conclusions

We here presented radiocarbon time series of the Atlantic thermocline ocean, which allows several important conclusions on the evolution of the Atlantic ventilation.

A consistent radiocarbon aging of thermocline waters occurred off Angola, at the equatorial Atlantic, and within the Southern Ocean, from which we infer a strong teleconnection of Southern Hemisphere thermocline waters during the last glacial. Simultaneously recorded abrupt shifts of B_{atm} ages highlight the strong glacial dynamic range of mid-depth ventilation and could indicate short periods of injection of aged deep water likely from the Pacific Ocean. The synchronous pattern of the Southern Hemisphere thermocline waters reveals that Angola thermocline water ages represents the "young" envelop of the strong age depth gradients, which provides a possibility to use the Angola record as a best guess of a Southern Hemisphere surface water calibration curve. In addition, the LSG model agrees well with the observed radiocarbon trends.

During the LGM and deglaciation, the thermoclines of the Atlantic north and south of the AF acted separately. Radiocarbon reconstructions from North Atlantic thermocline dwelling corals show mostly well-ventilated water. Our data further supports a southward shift of the AF and CVFZ as the most likely reason for the observed separation. Here, the LSG model mostly overestimates the role of southern sourced thermocline and intermediate waters in the regions of the AFC and Mauritania.

CWCs from Mauritania are sensitive to meridional water mass property change, due to their proximity to both the AF and CVFZ. Throughout the LGM, Mauritania is under the influence of ^{14}C rich water from northern sources contrasting the modern influence of southern sourced waters. The change to an Atlantic wide well-ventilated modern state of the thermocline waters and a more northern position of the AF and CVFZ occurred during the B/A period of initial Northern Hemisphere warming.

Lastly, further evidence of enhanced ocean ventilation during the B/A was found, with a clear meridional B_{atm} age difference of waters north and south of the AF of ~250 ± 50 years. Our data indicates a five century long in-situ aging of the Atlantic north of the AF followed by a resumption of ventilation in the middle of the YD at 12.5 ka to reach a modern subtropical Atlantic ventilation state by the end of the YD.

Data Availability Statement

All data associated to this article can be found at Beisel et al. (2023).

References

Adkins, J. F. (2013). The role of deep ocean circulation in setting glacial climates. *Paleoceanography*, *28*(3), 539–561. https://doi.org/10.1002/palo.20046

Adkins, J. F., Cheng, H., Boyle, E. A., Druffel, E. R. M., & Edwards, R. L. (1998). Deep-sea coral evidence for rapid change in ventilation of the deep North Atlantic 15,400 years ago. *Science*, *280*(5364), 725–728. https://doi.org/10.1126/science.280.5364.725

Andersen, M., Stirling, C., Zimmermann, B., & Halliday, A. (2010). Precise determination of the open ocean $^{234}U/^{238}U$ composition. *Geochemistry, Geophysics, Geosystems*, *11*(12), Q12003. https://doi.org/10.1029/2010GC003318

Barker, S., Knorr, G., Vautravers, M. J., Diz, P., & Skinner, L. C. (2010). Extreme deepening of the Atlantic overturning circulation during deglaciation. *Nature Geoscience*, *3*(8), 567–571. https://doi.org/10.1038/NGEO921

Barnola, J. M., Raynaud, D., Korotkevich, Y. S., & Lorius, C. (1987). Vostok ice core provides 160,000-year record of atmospheric CO_2. *Nature*, *329*(6138), 408–414. https://doi.org/10.1038/329408a0

Bazin, L., Landais, A., Lemieux-Dudon, B., Toyé Mahamadou Kele, H., Veres, D., Parrenin, F., et al. (2013). Delta ^{18}O measured on ice core NGRIP on AICC2012 chronology. *PANGAEA*. https://doi.org/10.1594/PANGAEA.824889

Beisel, E., Frank, N., Robinson, L. F., Lausecker, M., Friedrich, R., Therre, S., et al. (2023). Cold-water coral Atlantic thermocline ventilation records over the last 32.000 years [Dataset]. PANGAEA. https://doi.org/10.1594/PANGAEA.959508

Bereiter, B., Eggleston, S., Schmitt, J., Nehrbass-Ahles, C., Stocker, T. F., Fischer, H., et al. (2015). Revision of the EPICA Dome C CO_2 record from 800 to 600 kyr before present. *Geophysical Research Letters*, *42*(2), 542–549. https://doi.org/10.1002/2014GL061957

Böhm, E., Lippold, J., Gutjahr, M., Frank, M., Blaser, P., Antz, B., et al. (2015). Strong and deep Atlantic meridional overturning circulation during the last glacial cycle. *Nature*, *517*(7532), 73–76. https://doi.org/10.1038/nature14059

Bradtmiller, L. I., McManus, J. F., & Robinson, L. F. (2014). $^{231}Pa/^{230}Th$ evidence for a weakened but persistent Atlantic meridional overturning circulation during Heinrich Stadial 1. *Nature Communications*, *5*, 5817. https://doi.org/10.1038/ncomms6817

Burke, A., & Robinson, L. F. (2012). The Southern Ocean's role in carbon exchange during the last deglaciation. *Science*, *335*(6068), 557–561. https://doi.org/10.1126/science.1208163

Butzin, M., Prange, M., & Lohmann, G. (2005). Radiocarbon simulations for the glacial ocean: The effects of wind stress, Southern Ocean sea ice and Heinrich events. *Earth and Planetary Science Letters*, *235*(1–2), 45–61. https://doi.org/10.1016/j.epsl.2005.03.003

Carlson, A. E., & Clark, P. U. (2012). Ice sheet sources of sea level rise and freshwater discharge during the last deglaciation. *Reviews of Geophysics*, *50*(4), RG4007. https://doi.org/10.1029/2011RG000371

Chen, T., Robinson, L. F., Beasley, M. P., Claxton, L. M., Andersen, M. B., Gregoire, L. J., et al. (2016). Ocean mixing and ice-sheet control of seawater ^{234}U/^{238}U during the last deglaciation. *Science*, *354*(6312), 626–629. https://doi.org/10.1126/science.aag1015

Chen, T., Robinson, L. F., Burke, A., Claxton, L., Hain, M. P., Li, T., et al. (2020). Persistently well-ventilated intermediate-depth ocean through the last deglaciation. *Nature Geoscience*, *13*(11), 733–738. https://doi.org/10.1038/s41561-020-0638-6

Chen, T., Robinson, L. F., Burke, A., Southon, J., Spooner, P., Morris, P. J., & Ng, H. C. (2015). Synchronous centennial abrupt events in the ocean and atmosphere during the last deglaciation. *Science*, *349*(6255), 1537–1541. https://doi.org/10.1126/science.aac6159

Cheng, H., Edwards, R. L., Shen, C.-C., Polyak, V. J., Asmerom, Y., Woodhead, J., et al. (2013). Improvements in ^{230}Th dating, ^{230}Th and ^{234}U half-life values, and U–Th isotopic measurements by multi-collector inductively coupled plasma mass spectrometry. *Earth and Planetary Science Letters*, *371*, 82–91. https://doi.org/10.1016/j.epsl.2013.04.006

Chutcharavan, P. M., Dutton, A., & Ellwood, M. (2018). Seawater ^{234}U/^{238}U recorded by modern and fossil corals. *Geochimica et Cosmochimia Acta*, *224*, 1–17. https://doi.org/10.1016/j.gca.2017.12.017

Clauzet, G., Wainer, I., Lazar, A., Brady, E., & Otto-Bliesner, B. (2007). A numerical study of the South Atlantic circulation at the Last Glacial Maximum. *Palaeogeography, Palaeoclimatology, Palaeoecology*, *253*(3–4), 509–528. https://doi.org/10.1016/j.palaeo.2007.06.018

Cléroux, C., de Menocal, P., & Guilderson, T. (2011). Deglacial radiocarbon history of tropical Atlantic thermocline waters: Absence of CO_2 reservoir purging signal. *Quaternary Science Reviews*, *30*(15–16), 1875–1882. https://doi.org/10.1016/j.quascirev.2011.04.015

Curry, W. B., & Oppo, D. W. (2005). Glacial water mass geometry and the distribution of δ^{13}C of ΣCO_2 in the western Atlantic Ocean. *Paleoceanography*, *20*(1), PA1017. https://doi.org/10.1029/2004PA001021

Dubois-Dauphin, Q., Bonneau, L., Colin, C., Montero-Serrano, J. C., Montagna, P., Blamart, D., et al. (2016). South Atlantic intermediate water advances into the north-east Atlantic with reduced Atlantic meridional overturning circulation during the last glacial period. *Geochemistry, Geophysics, Geosystems*, *17*(6), 2336–2353. https://doi.org/10.1002/2016GC006281

Eltgroth, S. F., Adkins, J. F., Robinson, L. F., Southon, J., & Kashgarian, M. (2006). A deep-sea coral record of North Atlantic radiocarbon through the Younger Dryas: Evidence for intermediate water/deepwater reorganization. *Paleoceanography*, *21*(4), PA4207. https://doi.org/10.1029/2005PA001192

Fentimen, R., Feenstra, E., Rüggeberg, A., Vennemann, T., Hajdas, I., Adatte, T., et al. (2020). Cold-water coral mound archive provides unique insights into intermediate water mass dynamics in the Alboran Sea during the last deglaciation. *Frontiers in Marine Science*, *7*, 354. https://doi.org/10.3389/fmars.2020.00354

Frank, N., Hebbeln, D., Blaser, P., Carreiro-Silva, M., Diekamp, V., Eichstädter, R., et al. (2018). *ATHENA. Cruise No. M151—October 06, 2018-October 31, 2018-Ponta Delgada (Portugal)-Funchal (Portugal)*. Meteor-Berichte.

Frank, N., Paterne, M., Ayliffe, L., van Weering, T., Henriet, J.-P., & Blamart, D. (2004). Eastern North Atlantic deep-sea corals: Tracing upper intermediate water Δ^{14}C during the Holocene. *Earth and Planetary Science Letters*, *219*(3–4), 297–309. https://doi.org/10.1016/S0012-821X(03)00721-0

Franzese, A. M., Hemming, S. R., Goldstein, S. L., & Anderson, R. F. (2006). Reduced Agulhas Leakage during the Last Glacial Maximum inferred from an integrated provenance and flux study. *Earth and Planetary Science Letters*, *250*(1–2), 72–88. https://doi.org/10.1016/j.epsl.2006.07.002

Freeman, E., Skinner, L. C., Waelbroeck, C., & Hodell, D. (2016). Radiocarbon evidence for enhanced respired carbon storage in the Atlantic at the Last Glacial Maximum. *Nature Communications*, *7*(1), 1–8. https://doi.org/10.1038/ncomms11998

Heaton, T. J., Köhler, P., Butzin, M., Bard, E., Reimer, R. W., Austin, W. E., et al. (2020). Marine20—The marine radiocarbon age calibration curve (0–55,000 cal BP). *Radiocarbon*, *62*(4), 779–820. https://doi.org/10.1017/RDC.2020.68

Hebbeln, D., Wienberg, C., Bartels, M., Bergenthal, M., Frank, N., Gaide, S., et al. (2015). MoccoMeBo climate-driven development of Moroccan cold-water coral mounds revealed by MeBo-drilling: Atlantic vs. Mediterranean settings—Cruise MSM36—February 18–March 17, 2014–Malaga (Spain)–Las Palmas (Spain). In *MARIA S. MERIAN-Berichte, MSM, 36* (p. 47). https://doi.org/10.2312/cr_msm36

Hebbeln, D., Wienberg, C., Bender, M., Bergmann, F., Dehning, K., Dullo, W.-C., et al. (2017). *ANNA—Cold-water Coral Ecosystems off Angola and Namibia. Cruise M122-December 30, 2015-January 31, 2016-Walvisbay (Namibia)-Walvisbay (Namibia)*. Meteor-Berichte. https://doi.org/10.2312/cr_m122

Hesse, T., Butzin, M., Bickert, T., & Lohmann, G. (2011). A model-data comparison of δ^{13}C in the glacial Atlantic Ocean. *Paleoceanography*, *26*(3), PA3220. https://doi.org/10.1029/2010PA002085

Hines, S. K., Eiler, J. M., Southon, J. R., & Adkins, J. F. (2019). Dynamic intermediate waters across the late glacial revealed by paired radiocarbon and clumped isotope temperature records. *Paleoceanography and Paleoclimatology*, *34*(7), 1074–1091. https://doi.org/10.1029/2019PA003568

Hines, S. K., Southon, J. R., & Adkins, J. F. (2015). A high-resolution record of Southern Ocean intermediate water radiocarbon over the past 30,000 years. *Earth and Planetary Science Letters*, *432*, 46–58. https://doi.org/10.1016/j.epsl.2015.09.038

Hogg, A. G., Heaton, T. J., Hua, Q., Palmer, J. G., Turney, C. S., Southon, J., et al. (2020). SHCal20 Southern Hemisphere calibration, 0–55,000 years cal BP. *Radiocarbon*, *62*(4), 759–778. https://doi.org/10.1017/RDC.2020.59

Howe, J. N., Piotrowski, A. M., Noble, T. L., Mulitza, S., Chiessi, C. M., & Bayon, G. (2016). North Atlantic deep water production during the Last Glacial Maximum. *Nature Communications*, *7*(1), 1–8. https://doi.org/10.1038/ncomms11765

Huang, E., Mulitza, S., Paul, A., Groeneveld, J., Steinke, S., & Schulz, M. (2012). Response of eastern tropical Atlantic central waters to Atlantic meridional overturning circulation changes during the Last Glacial Maximum and Heinrich Stadial 1. *Paleoceanography*, *27*(3), PA3229. https://doi.org/10.1029/2012PA002294

Keigwin, L., & Schlegel, M. (2002). Ocean ventilation and sedimentation since the glacial maximum at 3 km in the western North Atlantic. *Geochemistry, Geophysics, Geosystems*, *3*(6), 1–14. https://doi.org/10.1029/2001GC000283

Keigwin, L. D. (2004). Radiocarbon and stable isotope constraints on Last Glacial Maximum and Younger Dryas ventilation in the western North Atlantic. *Paleoceanography*, *19*(4), PA4012. https://doi.org/10.1029/2004PA001029

Kerber, I. K., Arps, J., Eichstädter, R., Kontor, F., Dornick, C., Schröder-Ritzrau, A., et al. (2023). Simultaneous U and Th isotope measurements for U-series dating using MCICPMS. *Nuclear Instruments and Methods in Physics Research Section B: Beam Interactions with Materials and Atoms*, *539*, 169–178. https://doi.org/10.1016/j.nimb.2023.04.003

Kipp, M. A., & Tissot, F. L. (2022). Inverse methods for consistent quantification of seafloor anoxia using uranium isotope data from marine sediments. *Earth and Planetary Science Letters*, *577*, 117240. https://doi.org/10.1016/j.epsl.2021.117240

Köhler, P., Nehrbass-Ahles, C., Schmitt, J., Stocker, T. F., & Fischer, H. (2017). A 156 kyr smoothed history of the atmospheric greenhouse gases CO_2, CH_4, and N_2O and their radiative forcing. *Earth System Science Data*, *9*(1), 363–387. https://doi.org/10.5194/essd-9-363-2017

Krengel, T. (2020). *550,000 years of marine climate variability in the western Mediterranean Sea revealed by cold-water corals* (Dissertation). Heidelberg University.

Kromer, B., Lindauer, S., Synal, H.-A., & Wacker, L. (2013). MAMS—A new AMS facility at the Curt-Engelhorn-Centre for Achaeometry, Mannheim, Germany. *Nuclear Instruments and Methods in Physics Research Section B: Beam Interactions with Materials and Atoms*, *294*, 11–13. https://doi.org/10.1016/j.nimb.2012.01.015

Lambeck, K., Rouby, H., Purcell, A., Sun, Y., & Sambridge, M. (2014). Sea level and global ice volumes from the Last Glacial Maximum to the Holocene. *Proceedings of the National Academy of Sciences*, *111*(43), 15296–15303. https://doi.org/10.1073/pnas.1411762111

Lauvset, S. K., Lange, N., Tanhua, T., Bittig, H. C., Olsen, A., Kozyr, A., et al. (2021). An updated version of the global interior ocean biogeochemical data product, GLODAPv2. 2021. *Earth System Science Data*, *13*(12), 5565–5589. https://doi.org/10.5194/essd-13-5565-2021

Li, T., Robinson, L. F., Chen, T., Wang, X. T., Burke, A., Rae, J. W., et al. (2020). Rapid shifts in circulation and biogeochemistry of the Southern Ocean during deglacial carbon cycle events. *Science Advances*, *6*(42), eabb3807. https://doi.org/10.1126/sciadv.abb3807

Lippold, J., Luo, Y., Francois, R., Allen, S. E., Gherardi, J., Pichat, S., et al. (2012). Strength and geometry of the glacial Atlantic Meridional overturning circulation. *Nature Geoscience*, *5*(11), 813–816. https://doi.org/10.1038/ngeo1608

Lippold, J., Pöppelmeier, F., Süfke, F., Gutjahr, M., Goepfert, T. J., Blaser, P., et al. (2019). Constraining the variability of the Atlantic meridional overturning circulation during the Holocene. *Geophysical Research Letters*, *46*(20), 11338–11346. https://doi.org/10.1029/2019GL084988

Lohmann, G., & Lorenz, S. (2000). On the hydrological cycle under paleoclimatic conditions as derived from AGCM simulations. *Journal of Geophysical Research*, *105*(D13), 17417–17436. https://doi.org/10.1029/2000JD900189

Lozier, M. S. (1997). Evidence for large-scale eddy-driven gyres in the North Atlantic. *Science*, *277*(5324), 361–364. https://doi.org/10.1126/science.277.5324.361

Lund, D., Adkins, J., & Ferrari, R. (2011). Abyssal Atlantic circulation during the Last Glacial Maximum: Constraining the ratio between transport and vertical mixing. *Paleoceanography*, *26*(1), PA1213. https://doi.org/10.1029/2010PA001938

Lynch-Stieglitz, J., Adkins, J. F., Curry, W. B., Dokken, T., Hall, I. R., Herguera, J. C., et al. (2007). Atlantic meridional overturning circulation during the Last Glacial Maximum. *Science*, *316*(5821), 66–69. https://doi.org/10.1126/science.1137127

Maier-Reimer, E., Mikolajewicz, U., & Hasselmann, K. (1993). Mean circulation of the Hamburg LSG OGCM and its sensitivity to the thermohaline surface forcing. *Journal of Physical Oceanography*, *23*(4), 731–757. https://doi.org/10.1175/1520-0485(1993)023<0731:MCOTHL>2.0.CO;2

Mangini, A., Godoy, J. M., Godoy, M. L., Kowsmann, R., Santos, G. M., Ruckelshausen, M., et al. (2010). Deep sea corals off Brazil verify a poorly ventilated Southern Pacific ocean during H2, H1 and the Younger Dryas. *Earth and Planetary Science Letters*, *293*(3), 269–276. https://doi.org/10.1016/j.epsl.2010.02.041

Mangini, A., Lomitschka, M., Eichstädter, R., Frank, N., Vogler, S., Bonani, G., et al. (1998). Coral provides way to age deep water. *Nature*, *392*(6674), 347–348. https://doi.org/10.1038/32804

Marcott, S. A., Bauska, T. K., Buizert, C., Steig, E. J., Rosen, J. L., Cuffey, K. M., et al. (2014). Centennial-scale changes in the global carbon cycle during the last deglaciation. *Nature*, *514*(7524), 616–619. https://doi.org/10.1038/nature13799

McCulloch, M., Taviani, M., Montagna, P., Correa, M. L., Remia, A., & Mortimer, G. (2010). Proliferation and demise of deep-sea corals in the Mediterranean during the Younger Dryas. *Earth and Planetary Science Letters*, *298*(1–2), 143–152. https://doi.org/10.1016/j.epsl.2010.07.036

McManus, J. F., Francois, R., Gherardi, J. M., Keigwin, L. D., & Brown-Leger, S. (2004). Collapse and rapid resumption of Atlantic meridional circulation linked to deglacial climate changes. *Nature*, *428*(6985), 834–837. https://doi.org/10.1038/nature02494

Palma, C., Lillebø, A. I., Borges, C., Souto, M., Pereira, E., Duarte, A. C., & de Abreu, M. P. (2012). Water column characterisation on the Azores platform and at the sea mounts south of the archipelago. *Marine Pollution Bulletin*, *64*(9), 1884–1894. https://doi.org/10.1016/j.marpolbul.2012.06.015

Paul, A., & Schäfer-Neth, C. (2003). Modeling the water masses of the Atlantic Ocean at the Last Glacial Maximum. *Paleoceanography*, *18*(3), 1058. https://doi.org/10.1029/2002PA000783

Petit, J. R., Jouzel, J., Raynaud, D., Barkov, N. I., Barnola, J. M., Basile, I., et al. (1999). Climate and atmospheric history of the past 420,000 years from the Vostok ice core, Antarctica. *Nature*, *399*(6735), 429–436. https://doi.org/10.1038/20859

Prange, M., Lohmann, G., Romanova, V., & Butzin, M. (2004). Modelling tempo-spatial signatures of Heinrich events: Influence of the climatic background state. *Quaternary Science Reviews*, *23*(5–6), 521–527. https://doi.org/10.1016/j.quascirev.2003.11.004

Rafter, P. A., Gray, W. R., Hines, S. K., Burke, A., Costa, K. M., Gottschalk, J., et al. (2022). Global reorganization of deep-sea circulation and carbon storage after the last ice age. *Science Advances*, *8*(46), eabq5434. https://doi.org/10.1126/sciadv.abq5434

Reimer, P. J., Austin, W. E., Bard, E., Bayliss, A., Blackwell, P. G., Ramsey, C. B., et al. (2020). The IntCal20 Northern Hemisphere radiocarbon age calibration curve (0–55 cal kBP). *Radiocarbon*, *62*(4), 725–757. https://doi.org/10.1017/RDC.2020.41

Reimer, P. J., Baillie, M. G. L., Bard, E., Bayliss, A., Beck, J. W., Blackwell, P. G., et al. (2009). IntCal09 and Marine09 radiocarbon age calibration Curves, 0–50,000 years cal BP. *Radiocarbon*, *51*(4), 1111–1150. https://doi.org/10.1017/S0033822200034202

Reißig, S., Nürnberg, D., Bahr, A., Poggemann, D. W., & Hoffmann, J. (2019). Southward displacement of the North Atlantic subtropical gyre circulation system during North Atlantic cold spells. *Paleoceanography and Paleoclimatology*, *34*(5), 866–885. https://doi.org/10.1029/2018PA003376

Robinson, L. F., Adkins, J. F., Keigwin, L. D., Southon, J., Fernandez, D. P., Wang, S.-L., & Scheirer, D. S. (2005). Radiocarbon variability in the western North Atlantic during the last deglaciation. *Science*, *310*(5753), 1469–1473. https://doi.org/10.1126/science.1114832

Romero, O. E., Kim, J. H., & Donner, B. (2008). Submillennial-to-millennial variability of diatom production off Mauritania, NW Africa, during the last glacial cycle. *Paleoceanography*, *23*(3), PA3218. https://doi.org/10.1029/2008PA001601

Ruckelshausen, M. (2013). *Cold-water corals: A paleoceanographic archive; tracing past ocean circulation changes in the mid-depth subtropical western South Atlantic off Brazil for the last 40 ka BP* (Dissertation) Heidelberg University.

Schiebel, R., Schmuker, B., Alves, M., & Hemleben, C. (2002). Tracking the Recent and late Pleistocene Azores front by the distribution of planktic foraminifers. *Journal of Marine Systems*, *37*(1–3), 213–227. https://doi.org/10.1016/S0924-7963(02)00203-8

Schlitzer, R. (2023). Ocean data view. Retrieved from https://odv.awi.de

Schmittner, A. (2003). Southern Ocean sea ice and radiocarbon ages of glacial bottom waters. *Earth and Planetary Science Letters*, *213*(1–2), 53–62. https://doi.org/10.1016/S0012-821X(03)00291-7

Schröder-Ritzrau, A., Mangini, A., & Lomitschka, M. (2003). Deep-sea corals evidence periodic reduced ventilation in the North Atlantic during the LGM/Holocene transition. *Earth and Planetary Science Letters*, *216*(3), 399–410. https://doi.org/10.1016/S0012-821X(03)00511-9

Sigman, D. M., & Boyle, E. A. (2000). Glacial/interglacial variations in atmospheric carbon dioxide. *Nature*, *407*(6806), 859–869. https://doi.org/10.1038/35038000

Skinner, L., & Bard, E. (2022). Radiocarbon as a dating tool and tracer in paleoceanography. *Reviews of Geophysics*, *60*(1), e2020RG000720. https://doi.org/10.1029/2020RG000720

Skinner, L., Freeman, E., Hodell, D., Waelbroeck, C., Vazquez Riveiros, N., & Scrivner, A. (2021). Atlantic Ocean ventilation changes across the last deglaciation and their carbon cycle implications. *Paleoceanography and Paleoclimatology*, *36*(2), e2020PA004074. https://doi.org/10.1029/2020PA004074

Skinner, L., Primeau, F., Freeman, E., de la Fuente, M., Goodwin, P., Gottschalk, J., et al. (2017). Radiocarbon constraints on the glacial ocean circulation and its impact on atmospheric CO$_2$. *Nature Communications*, *8*(1), 1–10. https://doi.org/10.1038/ncomms16010

Skinner, L., & Shackleton, N. (2004). Rapid transient changes in northeast Atlantic deep water ventilation age across Termination I. *Paleoceanography*, *19*(2), PA2005. https://doi.org/10.1029/2003PA000983

Skinner, L. C., Waelbroeck, C., Scrivner, A. E., & Fallon, S. J. (2014). Radiocarbon evidence for alternating northern and southern sources of ventilation of the deep Atlantic carbon pool during the last deglaciation. *Proceedings of the National Academy of Sciences*, *111*(15), 5480–5484. https://doi.org/10.1073/pnas.1400668111

Slowey, N. C., & Curry, W. B. (1992). Enhanced ventilation of the North Atlantic subtropical gyre thermocline during the last glaciation. *Nature*, *358*(6388), 665–668. https://doi.org/10.1038/358665a0

Smith, J. E., Risk, M. J., Schwarcz, H. P., & McConnaughey, T. A. (1997). Rapid climate change in the North Atlantic during the Younger Dryas recorded by deep-sea corals. *Nature*, *386*(6627), 818–820. https://doi.org/10.1038/386818a0

Stanford, J. D., Rohling, E. J., Hunter, S. E., Roberts, A. P., Rasmussen, S. O., Bard, E., et al. (2006). Timing of meltwater pulse 1a and climate responses to meltwater injections. *Paleoceanography*, *21*(4), PA4103. https://doi.org/10.1029/2006PA001340

Struve, T., Wilson, D. J., Hines, S. K., Adkins, J. F., & van de Flierdt, T. (2022). A deep Tasman outflow of Pacific waters during the last glacial period. *Nature Communications*, *13*(1), 3763. https://doi.org/10.1038/s41467-022-31116-7

Stuiver, M., & Polach, H. A. (1977). Discussion reporting of ^{14}C data. *Radiocarbon*, *19*(3), 355–363. https://doi.org/10.1017/S0033822200003672

Sweeney, C., Gloor, E., Jacobson, A. R., Key, R. M., McKinley, G., Sarmiento, J. L., & Wanninkhof, R. (2007). Constraining global air-sea gas exchange for CO$_2$ with recent bomb ^{14}C measurements. *Global Biogeochemical Cycles*, *21*(2), GB2015. https://doi.org/10.1029/2006GB002784

Synal, H.-A., Stocker, M., & Suter, M. (2007). MICADAS: A new compact radiocarbon AMS system. *Nuclear Instruments and Methods in Physics Research Section B: Beam Interactions with Materials and Atoms*, *259*(1), 7–13. https://doi.org/10.1016/j.nimb.2007.01.138

Therre, S., Proß, L., Friedrich, R., Trüssel, M., & Frank, N. (2021). Heidelberg radiocarbon lab—Establishing a new carbon dioxide extraction line for carbonate samples. *Radiocarbon*, *63*, 1–10. https://doi.org/10.1017/RDC.2021.28

Thiagarajan, N., Subhas, A. V., Southon, J. R., Eiler, J. M., & Adkins, J. F. (2014). Abrupt pre-Bølling–Allerød warming and circulation changes in the deep ocean. *Nature*, *511*(7507), 75–78. https://doi.org/10.1038/nature13472

Thornalley, D. J., Barker, S., Broecker, W. S., Elderfield, H., & McCave, I. N. (2011). The deglacial evolution of North Atlantic deep convection. *Science*, *331*(6014), 202–205. https://doi.org/10.1126/science.1196812

Toggweiler, J., Dixon, K., & Bryan, K. (1989). Simulations of radiocarbon in a coarse-resolution world ocean model: 1. Steady state prebomb distributions. *Journal of Geophysical Research*, *94*(C6), 8217–8242. https://doi.org/10.1029/JC094iC06p08217

Trotter, J. A., McCulloch, M. T., D'Olivo, J. P., Scott, P., Tisnérat-Laborde, N., Taviani, M., & Montagna, P. (2022). Deep-water coral records of glacial and recent ocean-atmosphere dynamics from the Perth Canyon in the southeast Indian Ocean. *Quaternary Science Advances*, *6*, 100052. https://doi.org/10.1016/j.qsa.2022.100052

Van Rooij, D., Hebbeln, D., Comas, M., Vandorpe, T., & Delivet, S. T. M. S. S. (2013). EuroFLEETS Cruise summary report „MD194 GATE-WAY", Cádiz (ES) - Lissabon (PT), 10–21 June 2013.

Veitch, J., Penven, P., & Shillington, F. (2010). Modeling equilibrium dynamics of the Benguela current System. *Journal of Physical Oceanography*, *40*(9), 1942–1964. https://doi.org/10.1175/2010JPO4382.1

Waelbroeck, C., Duplessy, J.-C., Michel, E., Labeyrie, L., Paillard, D., & Duprat, J. (2001). The timing of the last deglaciation in North Atlantic climate records. *Nature*, *412*(6848), 724–727. https://doi.org/10.1038/35089060

WAIS. (2013). Onset of deglacial warming in West Antarctica driven by local orbital forcing. *Nature*, *500*(7463), 440–444. https://doi.org/10.1038/nature12376

WAIS. (2015). Precise interpolar phasing of abrupt climate change during the last ice age. *Nature*, *520*(7549), 661–665. https://doi.org/10.1038/nature14401

Wefing, A.-M., Arps, J., Blaser, P., Wienberg, C., Hebbeln, D., & Frank, N. (2017). High precision U-series dating of scleractinian cold-water corals using an automated chromatographic U and Th extraction. *Chemical Geology*, *475*, 140–148. https://doi.org/10.1016/j.chemgeo.2017.10.036

Westphal, H., Beuck, L., Braun, S., Freiwald, A., Hanebuth, T., Hetzinger, S., et al. (2014). *Phaeton-Paleoceanographic and paleo-climatic record on the Mauritanian Shelf—Cruise No. MSM16/3-October 13–November 20, 2010-Bremerhaven (Germany)—Mindelo (Cap Verde). MARIA S. MERIAN-Berichte, MSM16/3*. DFG-Senatskommission für Ozeanographie. https://doi.org/10.2312/cr_msm16_3

Wienberg, C., Titschack, J., Freiwald, A., Frank, N., Lundälv, T., Taviani, M., et al. (2018). The giant Mauritanian cold-water coral mound province: Oxygen control on coral mound formation. *Quaternary Science Reviews*, *185*, 135–152. https://doi.org/10.1016/j.quascirev.2018.02.012

Williams, T. J., Martin, E. E., Sikes, E., Starr, A., Umling, N. E., & Glaubke, R. (2021). Neodymium isotope evidence for coupled Southern Ocean circulation and Antarctic climate throughout the last 118,000 years. *Quaternary Science Reviews*, *260*, 106915. https://doi.org/10.1016/j.quascirev.2021.106915

Yu, J., Menviel, L., Jin, Z., Anderson, R., Jian, Z., Piotrowski, A., et al. (2020). Last glacial atmospheric CO$_2$ decline due to widespread Pacific deep-water expansion. *Nature Geoscience*, *13*(9), 628–633. https://doi.org/10.1038/s41561-020-0610-5